Daily denitrification rates in floodplains under contrasting pedo-climatic and anthropogenic contexts: modelling at the watershed scale

Clément Fabre, S. Sauvage, J. Guilhen, R. Cakir, M. Gerino, J. Sanchez-Perez

Daily denitrification rates in floodplains under contrasting pedo-climatic and anthropogenic contexts: modelling at the watershed scale

C. Fabre[1,*], S. Sauvage[1], J. Guilhen[1], R. Cakir[1], M. Gerino[1], J. M. Sánchez-Pérez[1]

[1] EcoLab, Université de Toulouse, CNRS, INPT, UPS, Toulouse, France

Corresponding author: Clément Fabre (clement.fabre21@gmail.com)

Abstract

Floodplains play a crucial role in water quality regulation via denitrification. This biogeochemical process reduces nitrate (NO_3^-), with aquifer saturation, organic carbon (OC) and N availability as the main drivers. To accurately describe the denitrification in the floodplain, it is necessary to better understand nitrate fluxes that reach these natural bioreactors and the transformation that occurs in these surface areas at the watershed scale. At this scale, several approaches tried to simulate denitrification contribution to nitrogen dynamics in study sites. However, these studies did not consider OC fluxes influences, hydrological dynamics and temperature variations at a daily time step. This paper focuses on a new model that allows insights on nitrate, OC, discharge and temperature influences on daily denitrification for each water body. We used a process-based deterministic model to estimate daily alluvial denitrification in different watersheds showing various pedo-climatic conditions. To better understand global alluvial denitrification variability, we applied the method to three contrasting catchments: The Amazon for tropical zones, the Garonne as representative of the temperate climate and the Yenisei for cold rivers. The Amazon with a high discharge, frequent flooding and warm temperature, leads to aquifers saturation, and stable OC concentrations. Those conditions favour a significant loss of N by denitrification. In the Garonne River, the low OC delivery limits the denitrification process. While Arctic rivers have high OC exports, the low nitrate concentrations and cold temperature in the Yenisei River hinder denitrification. We found daily alluvial denitrification rates of 119.4 ± 47.5, 7.6 ± 5.4 and 0.1 ± 0.5 $kgN.ha^{-1}.yr^{-1}$ during the 2000-2010 period for the Amazon, the Garonne and the Yenisei respectively. This study quantifies the floodplains influence in the water quality regulation service, their contribution to rivers geochemical processes facing global changes and their role on nitrate and OC fluxes to the oceans.

Keywords: denitrification; nitrate; floodplains; watershed; daily time step; organic carbon

1 Introduction

Intensive agriculture brings high amounts of nitrates to rivers by leaching of fertilizers. The nitrate concentrations in free river water are significantly lower than the nitrate concentrations in alluvial aquifers for areas under intense agriculture pressures (Sánchez-Pérez et al., 2003). This difference is explained by the dilution effect when the water flows from aquifers to rivers, together with the N retention capacity of floodplains (Craig et al., 2010). This retention capacity results from plant uptake and denitrification (Pinay et al., 1998; Craig et al., 2010; Ranalli and Macalady, 2010). Denitrification is the process of nitrate reduction (NO_3^-) into nitrous oxide (N_2O) or dinitrogen (N_2). It is the main process that leads to nitrate loss in watersheds (Pinay et al., 1998; Pfeiffer et al., 2006; Baillieux et al., 2014). Denitrifying bacteria are generally facultative aerobic heterotrophs (Zaman et al., 2012). They can switch to anaerobic respiration under low oxygen conditions by completing the denitrification, i.e. by using the oxygen from nitrate. Thus, denitrification is optimized under specific conditions and is limited by three main factors: the availability of nitrate, the availability of organic carbon (OC; Rivett et al., 2008) and the small oxygen availability (Zaman et al., 2012). In this way, denitrification is a microbial process consuming OC (Zaman et al., 2012). The OC used by denitrifying bacteria is taken from soils leaching and in-situ sediments or comes from the river contributions (Gift et al., 2010; Peter et al., 2012). OC in rivers is separated into two classes: particulate organic carbon (POC) and dissolved organic carbon (DOC; Hope et al., 1994). These two forms have two different origins. While POC mostly comes from soil erosion, DOC is a result of soil leaching (Meybeck, 1993; Raymond and Bauer, 2001). DOC is the most consumed OC form in denitrification (Peyrard et al., 2011; Zarnetske et al., 2011; Sun et al., 2018).

Floodplains are hot spots of denitrification (McClain et al., 2003; Billen et al., 2013). Floodplains are areas connected to the river network and are strongly influenced by the hydrodynamic of the basin, which results in oscillations between aerobic and anaerobic conditions. The location of floodplains intensifies transfers of OC and nitrate by leaching from uplands to the river. These transfers occur at hot moments with a high temporal resolution (Bernard-Jannin et al., 2017). Therefore, daily time step studies should highlight the temporal variability of the denitrification process.

Past studies used in situ observations to evaluate large-scale denitrification but they revealed high uncertainties (Groffman et al., 2006). Therefore, modelling appears as an important tool to better assess those processes at large scale (Groffman, 2012). Modelling tools that focus on the exchanges between rivers and floodplains were usually used for hydrology interactions (Yamazaki et al., 2011; Jung et al., 2012). Regarding floodplains biogeochemistry, previous models showed their ability to simulate denitrification (Hattermann et al., 2006; Sun et al., 2018). They can be used to identify nitrate sources and sinks (Boano et al., 2010; Peyrard et al., 2011; Zarnetske et al., 2012) as well as hot spots and hot moments of nutrients cycling (Groffman et al., 2009; Bernard-Jannin et al., 2017). Two options are commonly used to estimate denitrification at large scale: coupling a hydrological with biogeochemical models (Peyrard et al., 2011) or implementing biogeochemical modules in a hydrological model (Sun et al., 2018). Sun et al. (2018) was the first study to show models capacity to simulate daily denitrification variations at the scale of a reach by considering the river-aquifers exchanges of water, nitrate and OC. Denitrification is usually modelled as a nitrate retention rate (Boyer et al., 2006; Ruelland et al., 2007; Peyrard et al., 2011; Sun et al., 2018). Although the integration of the OC availability into floodplains denitrification is a recent effort (Sun et al., 2018), the temporal variations of OC fluxes have not been integrated into models yet. We assume that high temporal resolution of this OC delivery is important to consider in models as a control of the denitrification process. Thus, the accurate modelling approach to better simulate the effective biogeochemical processes with the limiting factors should be done at a daily time step.

Past research that uses modelling tools to predict spatial and temporal denitrification variations in floodplains highlighted the potential of these approaches to predict nitrate and OC fluxes at large scale (Peyrard et al., 2011; Bernard-Jannin et al., 2017; Sun et al., 2018). Recent research using new methods tried to estimate alluvial wetlands denitrification with remote sensing data (Guilhen et al., 2020). With a similar approach, this study is the first that aims to simulate denitrification at the scale of several watersheds with contrasting climatic and soil properties. The main objectives of the study are i) to propose a new and easy-to-use methodology to estimate floodplains denitrification at the watershed scale by taking into account spatial and temporal DOC variability, ii) to apply this methodology at the scale of three contrasting watersheds representative of various climatic and soils conditions and iii) to quantify their daily floodplains denitrification.

2 Materials and Methods

2.1 Study cases

To highlight the global denitrification variabilities, we selected three watersheds for their different ranges of nitrate and OC concentrations in the free waters. These three watersheds are the Amazon River, representative of tropical areas, with low nitrate and low OC content, the Yenisei River in Siberia, representative of cold climate, with low nitrate and high OC contents in the free-water, and the Garonne River in France, as a temperate and anthropogenic watershed, with high nitrate and low OC contents (Figure 1). Nitrate contents of the Amazon and the Yenisei rivers are mostly coming from natural sources while the Garonne basin shelters intensive agriculture activities. The Amazon basin is the largest draining area of the world with 6,500,000 km² and displays three large floodplains located in the Northern (the Branco Floodplain) and the Southern (the Madeira Floodplain) part of the basin as well as alongside the mainstream. Based on the GLOBAL-NEWS model results (Mayorga et al., 2010), the Amazon River has a dissolved inorganic nitrogen (DIN) export of 1.6 $kgN.ha^{-1}.yr^{-1}$ and a DOC export of 49.8 $kgC.ha^{-1}.yr^{-1}$. The DIN export consists mainly of nitrate, which is one of the compounds used in denitrification (Zaman et al., 2012). The basin also has an average soils OC content of 9 $kgC.m^{-3}$ (Batjes, 2009). The Yenisei River is one of the main rivers flowing into the Arctic Ocean with a basin area of 2,500,000 km². The main floodplains of the Yenisei River are in the downstream part of the main channel. The DIN export is around 0.3 $kgN.ha^{-1}.yr^{-1}$, the DOC export is at 10.6 $kgC.ha^{-1}.yr^{-1}$ while the average soils OC content is at 34 $kgC.m^{-3}$ (Batjes, 2009). Finally, the Garonne River is one of the main French basins with a draining area of 55,000 km². Wide floodplains are mainly located alongside the mainstream in the middle course. The DIN export of this river under high anthropogenic pressures is around 5.6 $kgN.ha^{-1}.yr^{-1}$ (Mayorga et al., 2010) with a DOC export of 14.3 $kgC.ha^{-1}.yr^{-1}$ and average soils OC content in soils of 9 $kgC.m^{-3}$.

2.2 Delineation of the floodplains

An accurate delineation of these areas (Figure 1) was performed to simulate the contribution of the floodplains at the watershed scale spatially. The Amazon and Yenisei floodplains were delineated based on the tools available in the new GIS-interface developed for the SWAT+ model (https://swat.tamu.edu/software/plus/). This method allows the user to delineate floodplains based on a slope threshold (Rathjens et al., 2015) with a digital elevation model (DEM) from de Ferranti and Hormann (2012). For the Garonne, this method was not able to return consistent delineation. Thus the Garonne floodplain boundaries were based on alluvial soils area (Fluvisols) as proposed by Sun et al. (2018).

Floodplains of the three watersheds cover over 660,000 km² (10.2%), 419,000 km² (15.5%), 4,000 km² (7.1%) for the Amazon, the Yenisei and the Garonne basins, respectively. Forests and pastures mainly cover Amazon and Yenisei floodplains with 78% and 13% for the Amazon and 66% and 20% for the Yenisei (Figure 1). Nevertheless, some areas are covered by agriculture, especially in the upstream parts of the watersheds. On the contrary, the Garonne floodplains are mostly covered by agriculture, with over 65% of the total area.

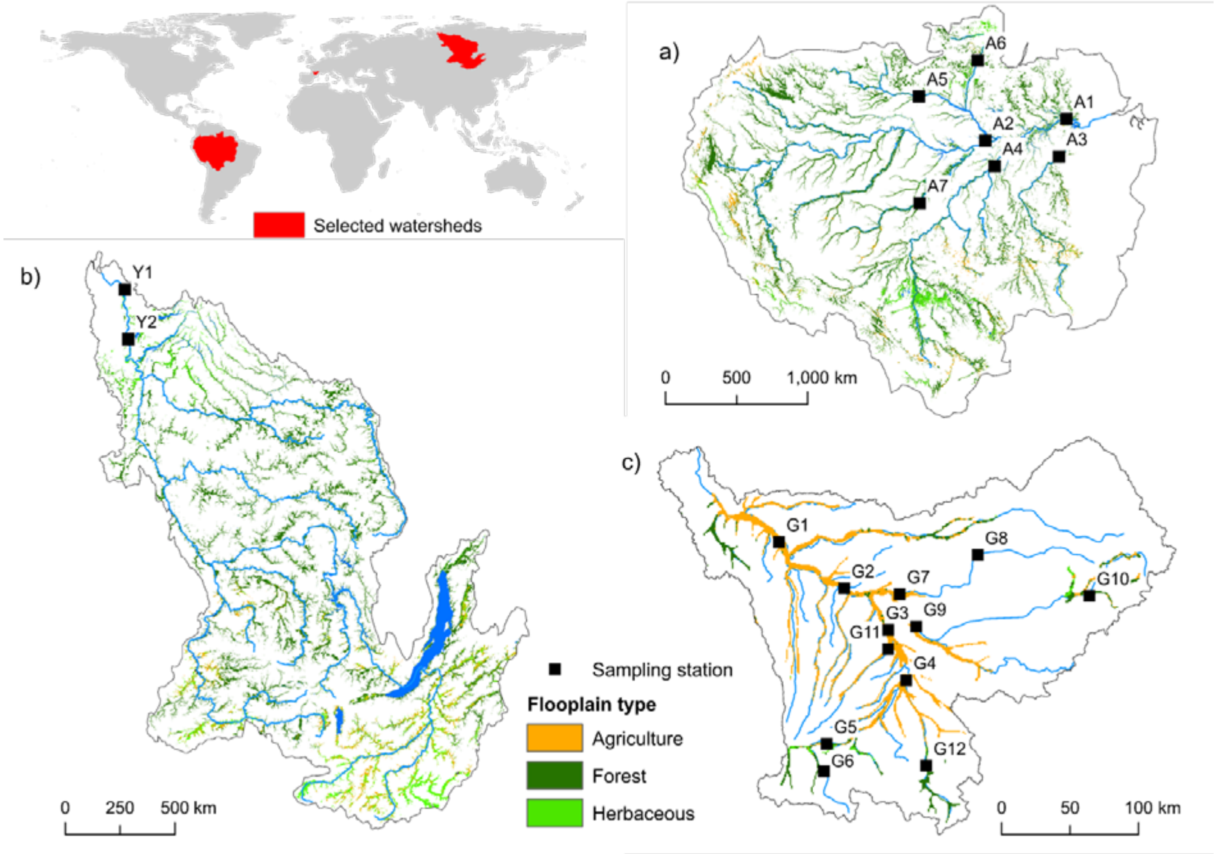

Figure 1: Study areas: a) The Amazon, b) The Yenisei and c) The Garonne rivers and their respective sampling stations used to calibrate the hydrology and the nutrients fluxes. Delineation of the floodplains was based on the method of Rathjens et al. (2015) and the Digital Elevation Model of de Ferranti and Hormann (2012) for the Amazon and the Yenisei rivers. For the Garonne River, floodplains delineation originate from on the soils database of Batjes (2009). Land covers came from the Global Land Cover Database 2000 (European Commission, 2003).

2.3 Model implementation for denitrification

The first model applied by Peyrard et al. (2011) estimated the denitrification rate in the hyporheic zone. This rate estimation depends on the availability of POC, DOC and NO_3^- as well as oxygen (O_2) availability and influence of nitrification rate from ammonia (NH_4^+) transformation. Sun et al. (2018) simplified the equation by removing the ammonia term and used surface water-groundwater exchanges to approach the anaerobic conditions. A focus on the soil water content is necessary to assess when anaerobic conditions are occurring to trigger denitrification (Sauvage et al., 2018; Sun et al., 2018).

Guilhen et al. (2020) used remote sensing data to assess the extent of water bodies as well as the water saturation in soils where denitrification occurs. Indeed, the denitrification rate in this study depends on the Surface Water Fraction (SWAF) product. Although this product possesses a low spatial resolution (25 km x 25 km for one pixel), its high frequency (3 days to map the whole Amazon Basin; Parrens et al., 2019) makes it possible to record a sudden change in the hydrology. By comparing the brightness temperature of forest and water, a percentage of water cover in a pixel was deduced and used to estimate the anaerobic conditions in the model of Peyrard et al. (2011). Nevertheless, the SWAF data determine the surface water extent in a pixel with a coarse resolution of 25 km x 25 km. However, the SWAF methodology had only been used on the Amazon River so far (Parrens et al., 2017; 2018; 2019) and remote sensing data used in this methodology are not available for Arctic zones yet.

In this study, we followed the conceptual schema shown in Figure 2 with denitrification occurring in the floodplain aquifers by using the available nitrate and OC content in aquifers.

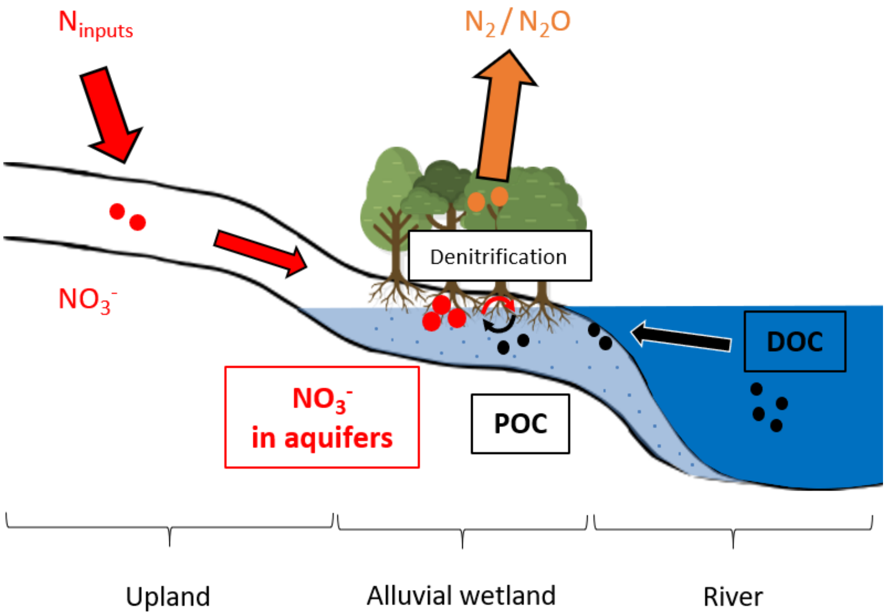

Figure 2: Conceptual representation of the denitrification in floodplains based on the previous studies of Sánchez-Pérez and Trémolières (2003), Sauvage et al. (2018) and Sun et al. (2018).

The denitrification process studied in past research is as followed:

$$4\,NO_3^- + 5\,CH_2O + 4\,H^+ \rightarrow 2\,N_2(g) + 5\,CO_2(g) + 7\,H_2O \qquad (1)$$

Abril and Frankignoulle (2001) demonstrated an increase in alkalinity due to wetland denitrification. To take this phenomenon into account, the formation of HCO_3^- from dissolved CO_2 (eq.2) was coupled to the denitrification (eq.1). Overall, in this study, denitrification was modelled using the following equation:

$$4\,NO_3^- + 5\,CH_2O \rightarrow 2\,N_2(g) + \,CO_2(g) + \,4\,HCO_3^- + \,3\,H_2O \qquad (2)$$

By using $x = 5$ in (2) to compare the use of organic carbon and the consumption or the production of the other molecules (Peyrard et al., 2011), we obtain:

$$0.8x\,NO_3^- + x\,CH_2O \rightarrow 0.5x\,N_2(g) + 0.2x\,CO_2(g) + \,0.8x\,HCO_3^- + \,0.6x\,H_2O \qquad (3)$$

Sun et al. (2018) showed the capability of Peyrard et al. (2011) model to describe the denitrification rates in the main floodplains of the Garonne by comparing their simulations with in-situ denitrification measurements. However, applying this model at the watershed scale or in other watersheds was not practicable because of its specific design for the middle course

Garonne floodplains. To further estimate denitrification in contrasting basins, we investigated a more straightforward method considering OC dynamics and anaerobic conditions.

Therefore, we applied a new version of the model allowing an estimation of the denitrification rate based on easy-to-obtain variables as followed:

$$R_{NO3,i} = -0.8x\left(\rho.\frac{1-\varphi}{\varphi}.k_{POC}[POC_i].\frac{10^6}{M_c} + k_{DOC}[DOC_i]\right).\frac{[NO_{3,i}]}{K_{NO_3} + [NO_{3,i}]}.\frac{Q_i}{Q_{bnk}}.e^{\frac{-(T_i - T_{opt})^2}{100}} \qquad (4)$$

where $R_{NO3,i}$ is the denitrification rate in µmol.L^{-1} on day *i*, $0.8x$ is the stoichiometric proportion of nitrate consumed in denitrification compared to the organic matter used with $x = 5$, ρ is the dry sediment density in kg.dm^{-3}, φ corresponds to the sediment porosity, k_{POC} and k_{DOC} are the mineralization rate constants of POC and DOC (day^{-1}), $[POC_i]$ and $[DOC_i]$ are the concentrations on day *i* (µmol.L^{-1}) of POC in alluvial soils and DOC in the river, M_c is the carbon molar mass (g.mol^{-1}), $[NO_{3,i}]$ is the nitrate concentration in the aquifer on day *i* (µmol.L^{-1}), K_{NO_3} is the half-saturation constant for nitrate limitation (µmol.L^{-1}), Q_i and Q_{bnk} are the discharge on day *i* and the discharge at bank full depth, T_i and T_{opt} are the temperature in the subbasin on day *i* and the optimal temperature for denitrification. T_{opt} was fixed to 27°C (Saad and Conrad, 1993; Canion et al., 2014; Brin et al., 2017). The stoichiometric ratio between the consumption of nitrate and OC in the denitrification is $0.8x$ as in (3). More details on the conceptualization of the model could be found in Peyrard et al. (2011).

Our global modelling strategy consists in the application of the former model (equation 4) with the help of N and C entry data coming from two different sources (Figure 3). Firstly, a generic model calculates the DOC concentrations in rivers, and secondly, the SWAT model estimates nitrate concentrations in aquifers. We correlated the daily DOC concentrations to the daily discharge with the relation proposed by Fabre et al. (2019) for the study case of the Yenisei River. We assumed that POC concentrations in soils are not profoundly affected in time. POC concentrations were considered much larger than the other nutrients involved in the denitrification model. Thus, we fixed the values of average POC content in soils for each watershed based on Batjes (2009).

DOC concentrations in the river and NO_3^- content in aquifers were extracted or calculated in each subbasin, as explained in the following paragraphs. Then, our model estimates the denitrification rate at a daily time step for each water body. Finally, these calculations helped to determine an average annual denitrification rate. Figure 3 summarizes our approach used to estimate the daily denitrification rate in the floodplains of the three watersheds.

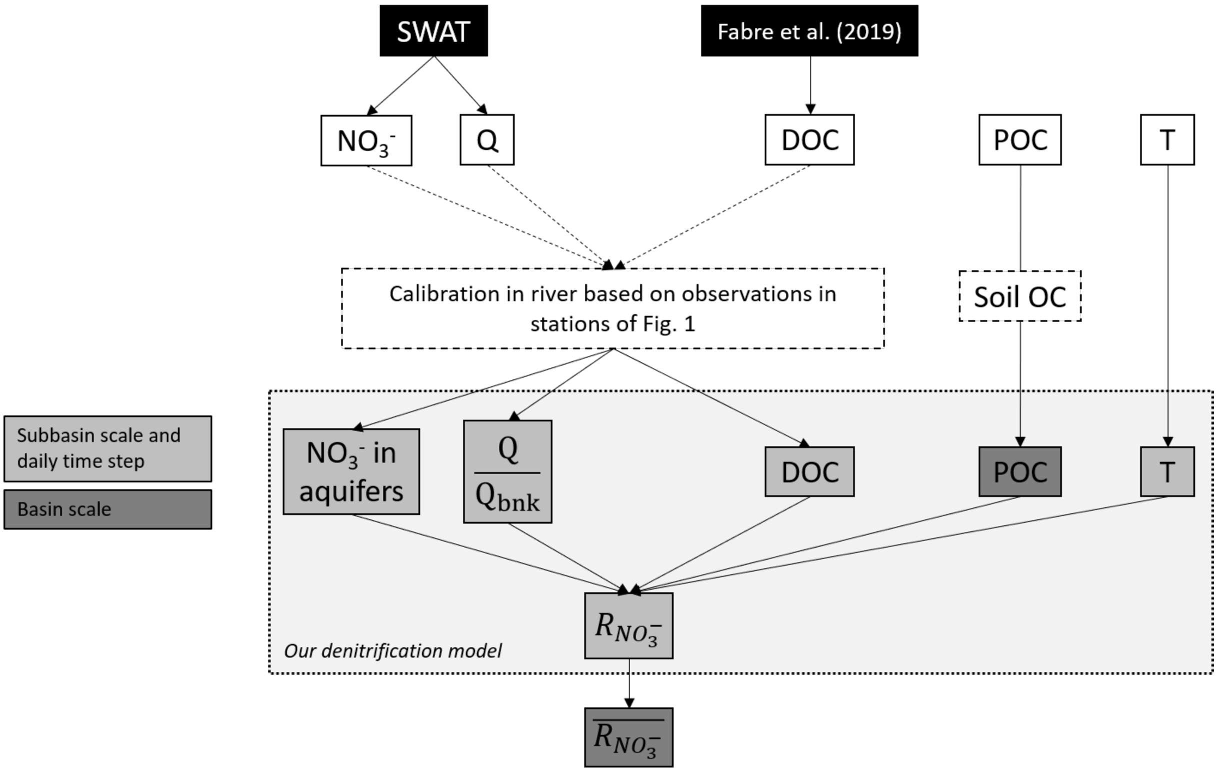

Figure 3: Details of the different steps of the denitrification model setup. First, the Soil and Water Assessment Tool (SWAT) and the Fabre et al. (2019) model are calibrated to estimate discharge and riverine nutrients concentrations. Then, these results are used to follow nutrients contents in floodplains aquifers and to calculate the denitrification rate.

Denitrifying bacteria are more efficient at an optimal temperature of around 25-30°C (Saad and Conrad, 1993; Canion et al., 2014; Brin et al., 2017). Therefore a temperature term following a Gaussian function with an optimum was added into the model of Sun et al. (2018) to better describe the denitrification variability according to the watersheds with various climates.

We fixed the half-saturation constant for nitrate limitation based on Peyrard et al. (2011) estimations in the hyporheic zone from in-field measurements. The two OC mineralization rate constants were calculated by Sun et al. (2018) based on in-situ observations on the Garonne

River. These two parameters integrate the temperature effect on the microbial ability to degrade the organic matter. New k_{POC} and k_{DOC} values independent from the temperature allow exporting this calibration to the two other watersheds. These new values were obtained by dividing k_{POC} and k_{DOC} of Sun et al. (2018) by the temperature term of (4) filled with the average temperature in the Garonne watershed ($\overline{T}_{Garonne}$) as followed:

$$\begin{cases} k_{POC} = \dfrac{k_{POC,Sun\ et\ al.(2018)}}{e^{\frac{-(\overline{T}_{Garonne} - T_{opt})^2}{100}}} \\ \\ k_{DOC} = \dfrac{k_{DOC,Sun\ et\ al.(2018)}}{e^{\frac{-(\overline{T}_{Garonne} - T_{opt})^2}{100}}} \end{cases} \tag{5}$$

These new k_{POC} and k_{DOC} values were assumed valid to be used for the two other watersheds since the daily temperatures control the denitrification rates variations.

2.4 Model choice to estimate Nitrate and DOC dynamics

This study uses the Soil and Water Assessment Tool (SWAT) model to assess and quantify nitrate and OC dynamics based on discharge simulations of the three selected watersheds. SWAT is a hydro-agro-climatological model developed by USDA Agricultural Research Service (USDA-ARS; Temple, TX, USA) and Texas A&M AgriLife Research (College Station, TX, USA; Arnold et al., 1998). Its performance has already been tested at multiple catchment scales in various climatic and soil conditions on water, sediment and water chemistry especially nitrogen (Fu et al., 2019) and organic carbon (Oeurng et al., 2011) exports. Theory and details of hydrological and water quality processes integrated into SWAT are available online (http://swatmodel.tamu.edu/). For the Garonne River, we integrated most of the anthropogenic pressures in the basin to represent the watershed dynamics. Irrigation and dam management were implemented into the modelling based on national surveys from CACG (https://www.cacg.fr/fr/) and Electricité de France (REGARD-RTRA/STAE program). In the same way, city effluents were calibrated based on European databases of UWWTP – EUDB

(EEA Report, 2013; https://ec.europa.eu/). Finally, land-use databases were updated to better simulate the fertilizers supply in the basin and to better match with national crop yields, as demonstrated in Cakir et al. (2020). The SWAT model integrates the nitrogen cycle. SWAT calculates the denitrification in soils but does not consider the denitrification occurring in aquifers.

The nitrogen cycle in SWAT was calibrated with observed in-stream nitrate concentrations available at the different gauging stations shown in Figure 1. Based on the correlation between observed and simulated concentrations during low flow periods, we assumed that simulated nitrate concentrations in aquifers are representative of real conditions. Thus, the nitrate concentrations in aquifers, as new denitrification model inputs (equation 4), were extracted from the SWAT model at the subbasin scale and at a daily time step. Concerning the anaerobic conditions, as it was demonstrated in Sun (2015), the denitrification rate is linked to the water volume stored in floodplains aquifers. The latter is linked to the water level in the channel (Helton et al., 2014; Sun et al., 2018). Therefore, we considered a ratio between the daily discharge in the stream extracted from SWAT and the discharge at bank full depth. The ratio is limited to 1 and depicts the gap between the current discharge and the discharge needed to produce a flooding. It is linked to the aquifers filling and trigger denitrification when it is close to 1. SWAT accurately simulates the discharges at different time steps and at small or large scales (Ferrant et al., 2011; Lu et al., 2019). However, the SWAT model encounters difficulties to estimate discharges at bank full depth with accuracy due to the different resolutions of the Digital Elevation Models (DEMs) used. Based on rating curves in gauging stations of the three watersheds, we adjusted the value of the discharge at bank full depth (Q_{bnk}) to allow better variations of the Q_i/Q_{bnk} ratio in time and space. We used ratios of 7/8, 1/5 and 1/4 to refine bank full depth discharges for the Amazon, the Garonne and the Yenisei, respectively. Consequently, bank full depth discharges were changed from 262,000 $m^3.s^{-1}$ to around 200,000 $m^3.s^{-1}$ at Obidos for the Amazon River, from 7,700 $m^3.s^{-1}$ to 640 $m^3.s^{-1}$ at Verdun for the Garonne River and from above 1,400,000 $m^3.s^{-1}$ to 140,000 $m^3.s^{-1}$ at Dudinka for the Yenisei River.

2.5 Hydrology calibration

Hydrology was first manually calibrated. Then an automatic calibration with three loops of 500 calibrations was done on the Yenisei and the Garonne basins as evoked in Fabre et al. (2017) and Cakir et al. (2020) with the SWAT-CUP software. For the Amazon River, the hydrology was calibrated manually as for the OC and the nitrate dynamics. The calibration was performed with available observations in rivers extracted from the Observation Service SO HYBAM (https://hybam.obs-mip.fr/), the French Water Agency of the Garonne River (http://www.eau-adour-garonne.fr/) and the Arctic Great Rivers Observatory (Holmes et al., 2018) datasets for the Amazon, the Garonne and the Yenisei, respectively. For the Amazon, we calibrated and validated the model manually over the 2000-2009 period and the 2010-2016 period, respectively. For the Garonne, the model was calibrated from 2000 to 2005 and was validated from 2006 to 2010 based on Cakir et al. (2020). For the Yenisei, the model was calibrated over 2003 to 2010 and validated over the 2011-2016 period based on Fabre et al. (2019).

2.6 Validity of simulated Nitrate and DOC dynamics

We used two indices to validate our simulated riverine nitrate and DOC concentrations with observed data: the coefficient of determination (R^2) and the percentage of bias (PBIAS). These indices are detailed in Moriasi et al. (2007). R^2 ranges from 0 to 1, with higher values indicating less error variance. R^2 higher than 0.3 could be considered acceptable for daily biogeochemical modelling (Moriasi et al., 2015). PBIAS expresses the percentage of deviation between simulations and observations. Thus, the optimal value is 0. PBIAS can be positive or negative, which reveals a model underestimation or overestimation bias, respectively (Moriasi et al., 2007).

2.7 Water quality efficiency ratio

We used an efficiency ratio R based on the exported fluxes out of the basin (F_{outlet}) to test the denitrification efficiency in the watershed. This ratio compares the nutrients flux consumed by denitrification (F_{denit}) to the total fluxes exported, e.g. exported at the watershed outlet and removed by denitrification:

$$R = \frac{F_{denit}}{F_{denit} + F_{outlet}} \tag{6}$$

3 Results

3.1 Nitrate and DOC simulations from SWAT in the three watersheds

The results of nitrate and DOC dynamics at the Amazon outlet are in the range of in-situ observations regarding the PBIAS index. Still, they show discrepancies with the temporal variations (Figure 4a and Figure 5a). On the Garonne River, the simulated nitrate concentrations are in the range of observations during high flow periods but display underestimations during low flow periods (Figure 4b). Concerning DOC concentrations, the simulations are in agreement with the observations ranges on the three watersheds. They do not simulate the dynamics of observed data in the Garonne and Amazon rivers accurately (Figure 5). However, these simulations are conserved because the PBIAS index and the p-values show that they are in the range of the observations with regards to the low number of observed data (Moriasi et al., 2015). Based on this assessment, the simulated DOC fluxes (Appendix 1) are assumed to describe the observed data adequately. In the same way, the good representation of low-water nitrate concentrations upstream to the floodplains indicates that the simulated nitrate content in the floodplains aquifers should be close to reality. Table 1 shows the fitted parameters used to obtain these theoretical C and N concentrations.

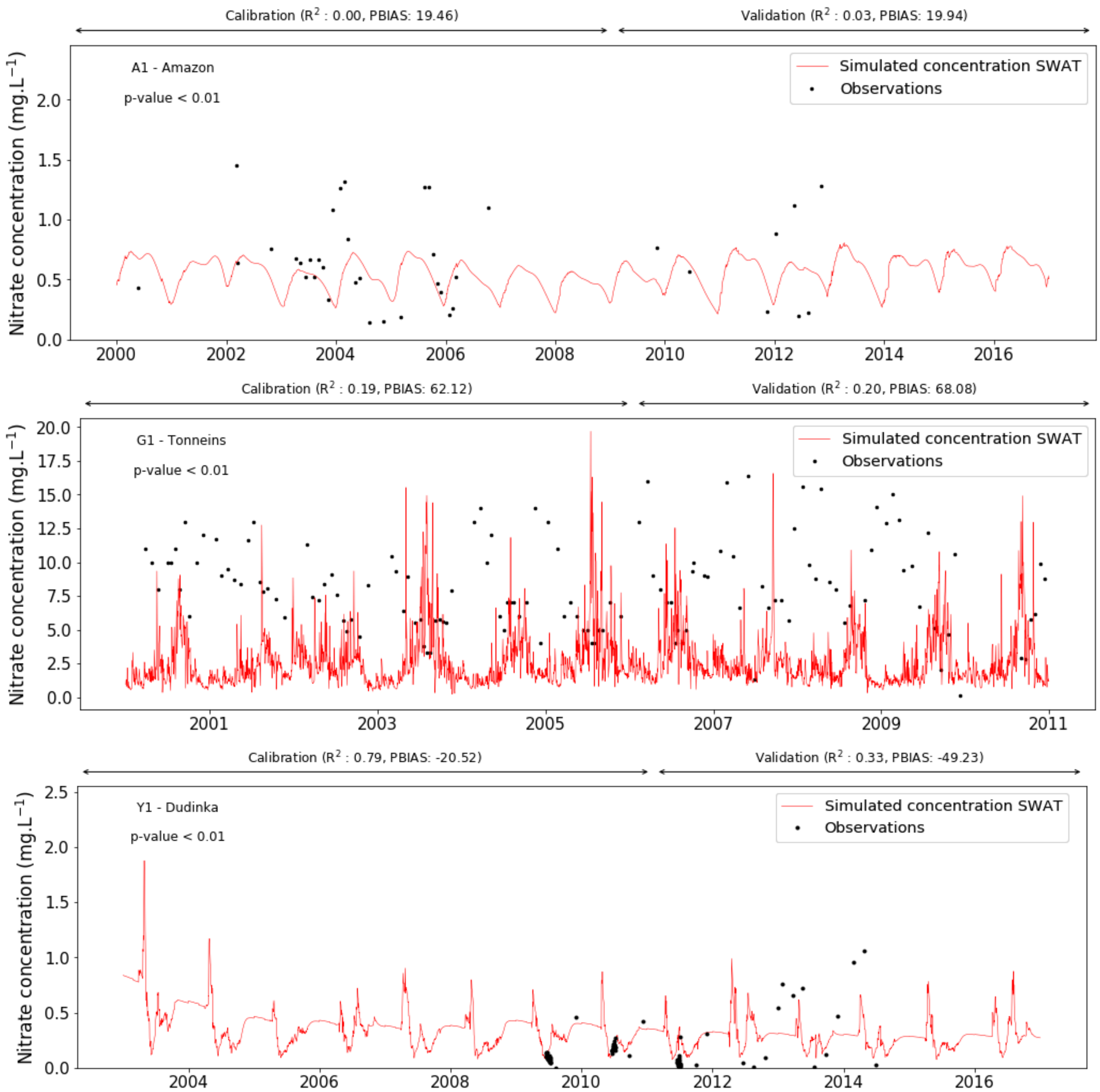

Figure 4: Daily observed and simulated nitrate concentrations (mg.L^{-1}) at the outlet of a) the Amazon, b) the Garonne and c) the Yenisei rivers. Locations of the sampling stations are found in Figure 1.

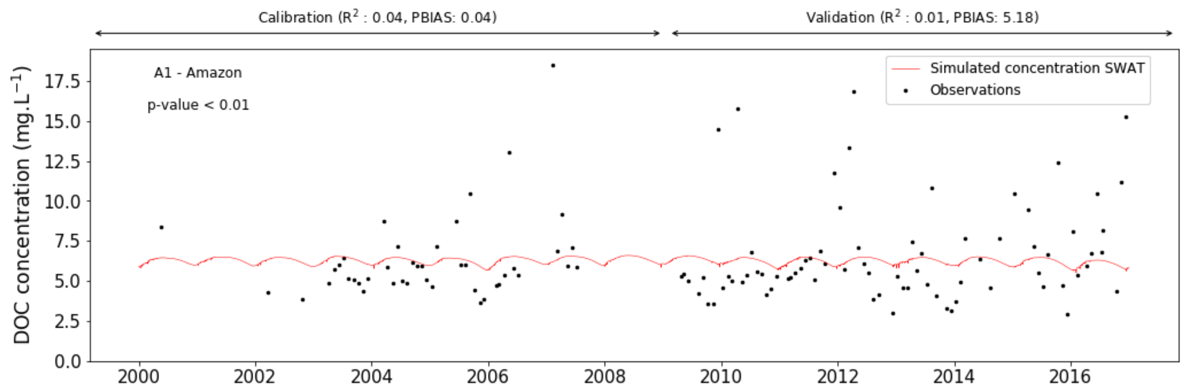

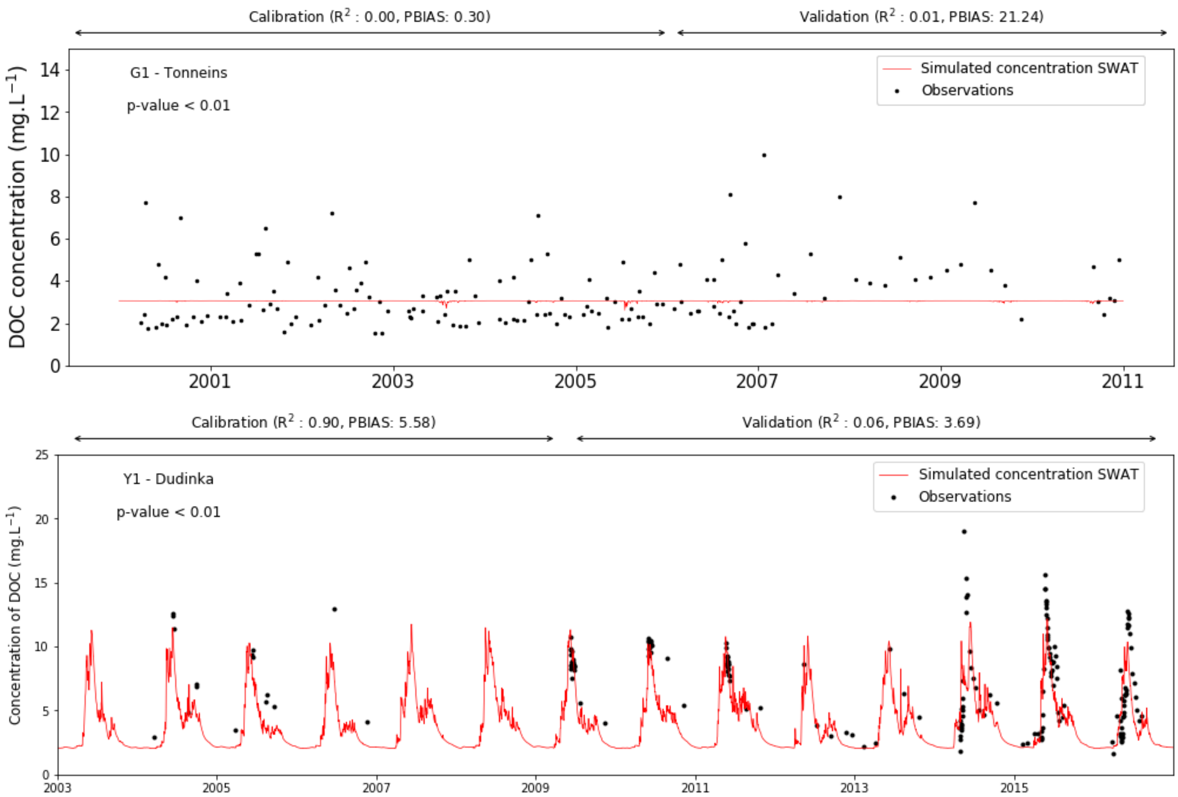

Figure 5: Daily observed and simulated DOC concentrations at the outlet of a) the Amazon, b) the Garonne and c) the Yenisei rivers. The Yenisei graph is adapted from Fabre et al. (2019). Locations of the sampling stations are found in Figure 1.

Table 1: Fitted values of the SWAT parameters for the three watersheds for nitrate and organic carbon. The parameters for the Amazon River were calibrated manually based on riverine observations from the Observation Service SO HYBAM. The settings for the Garonne and Yenisei Rivers were adapted from Cakir et al. (2020) and Fabre et al. (2019), respectively. The SWAT parameters linked to denitrification refer to the one in soils. SWAT does not integrate the denitrification occurring in floodplains aquifers.

				Value for:		
File	Parameter	Definition	Default	Amazon	Garonne	Yenisei
Nitrate parameters:						
*.bsn	CDN	Denitrification exponential rate coefficient	1.0	0.5	1.0	3.0
	CH_ONCO_BSN	Channel organic nitrogen concentration in channel (ppm)	0	0	25	0
	CMN	Rate factor for humus mineralization of active organic nitrogen	0.0003	0.06	0.001	0.06
	IWQ	In-stream water quality (QUAL2E module)	1	0	1	0
	N_PERCO	Nitrogen percolation coefficient	0.2	3	0.58	0
	N_UPDIS	Nitrogen uptake distribution parameter	20	20	40	20
	RSDCO	Residue decomposition coefficient	0.05	0.1	0.1	0.01
	SDNCO	Denitrification threshold water content in soils	1.1	1.1	1.5	0.8
*.chm	SOL_NO3	Initial nitrate concentration in the soil layer	0	0	19	0
	SOL_ORGN	Initial organic N concentration in the soil layer	0	0	30	0
*.swq	BC1	Rate constant for biological oxidation of NH3 in the reach at 20°C (1/day)	0.550	0.550	1	0.550
	BC2	Rate constant for biological oxidation of NO2 to NO3 in the reach at 20°C (1/day)	1.100	1.100	2	1.100
	BC3	Rate constant for biological oxidation of NO2 to NO3 in the reach at 20°C (1/day)	0.210	0.210	0.21	0.210
	RS4	Rate coefficient of organic N settling in the reach at 20°C (1/day)	0.050	0.050	0.001	0.050
*.wwq	AI1	Fraction of algal biomass that is nitrogen (mg N/mg alg)	0.08	0.08	0.09	0.08
Organic carbon:						
*.bsn *.sub	α	Potential maximum DOC concentration in the river ($mg.L^{-1}$)		5.72 – 12.43	2.10 – 3.38	15.0
	β	Discharge at which the DOC concentration equals half of α ($mm.day^{-1}$)		0.001 – 0.74	0.001 – 0.03	1.22

3.2 Simulated average denitrification rates in contrasting watersheds

With the help of the new denitrification model (exposed in Equation 4), the parameters detailed in Table 2 and the previous works on DOC exports, we were able to assess the floodplains denitrification rates for the three considered watersheds. The average annual rates of the floodplain denitrification are at 73.0 ± 6.2 kgN.ha^{-1}.yr^{-1} for the Amazon, 4.5 ± 1.4 kgN.ha^{-1}.yr^{-1} for the Garonne and 0.7 ± 0.2 kgN.ha^{-1}.yr^{-1} for the Yenisei.

Table 2: Calibrated values of the different parameters used in the floodplains denitrification rates calculations based on the work of Peyrard et al. (2011) and Sun et al. (2018) on the Garonne River.

Basin	Amazon	Garonne	Yenisei
ρ (kg.dm^{-3})	0.25	0.15	0.1
φ	1.03	1.3	1.03
k_{DOC} (day^{-1})	1.88.10^{-3}	3.63.10^{-3}	1.88.10^{-3}
k_{POC} (day^{-1})	2.75.10^{-4}		
$[POC]$ (µmol.L^{-1})	1	1.5	33
K_{NO_3} (µmol.L^{-1})	30		
T_{opt} (°C)	27		

Figure 6 shows the annual average denitrification fluxes in floodplains found in this study. It highlights the hot spots of denitrification for each of the three watersheds. The hot spots for the Amazon basin are located in the Northern part of the watershed. At the same time, the denitrification in the Garonne basin is usually higher in the primary active floodplains between the stations G3 and G4 but also in the upstream parts near G5 (see Figure 1 for stations locations). For the Yenisei watershed, the hotspots are located in the unfrozen parts of the basin and in the Lake Baikal.

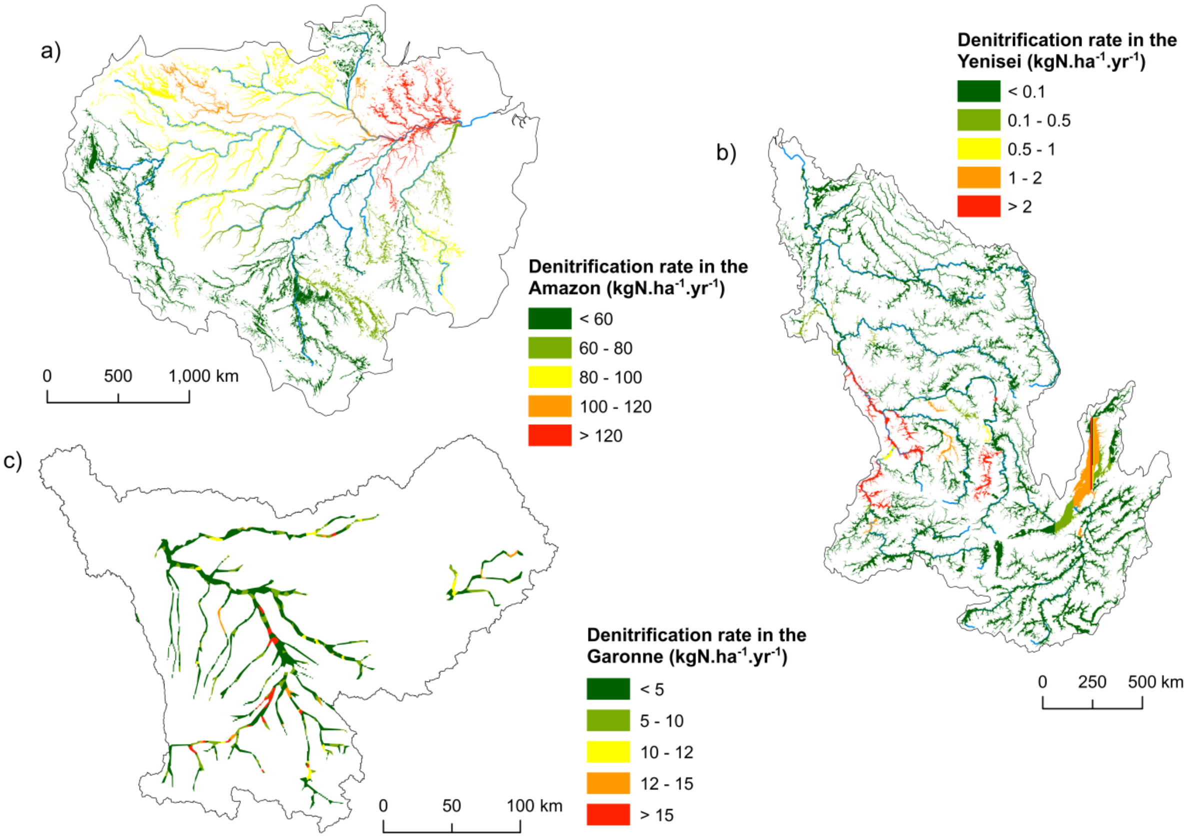

Figure 6: Representation of the mean annual average DOC consumption (kgC.ha^{-1}.yr^{-1}) in denitrification in floodplains of the three selected watersheds on the 2000-2010 period.

3.3 Temporal variability of the denitrification

Figure 7 shows the average daily denitrification rates (R_{NO3}) on the 2000-2010 period for the three watersheds. For the Amazon, R_{NO3} is maximal in April with a removal around 0.31 kgN.ha^{-1}.day^{-1}. The lowest values are around 0.09 kgN.ha^{-1}.day^{-1} in October. R_{NO3} reaches 0.06 kgN.ha^{-1}.day^{-1} in May on the Garonne and is lower during the cold season between October and February. With the same pattern, the Yenisei shows higher rates during the unfreezing period around May, but these rates are still low compared to the two other basins.

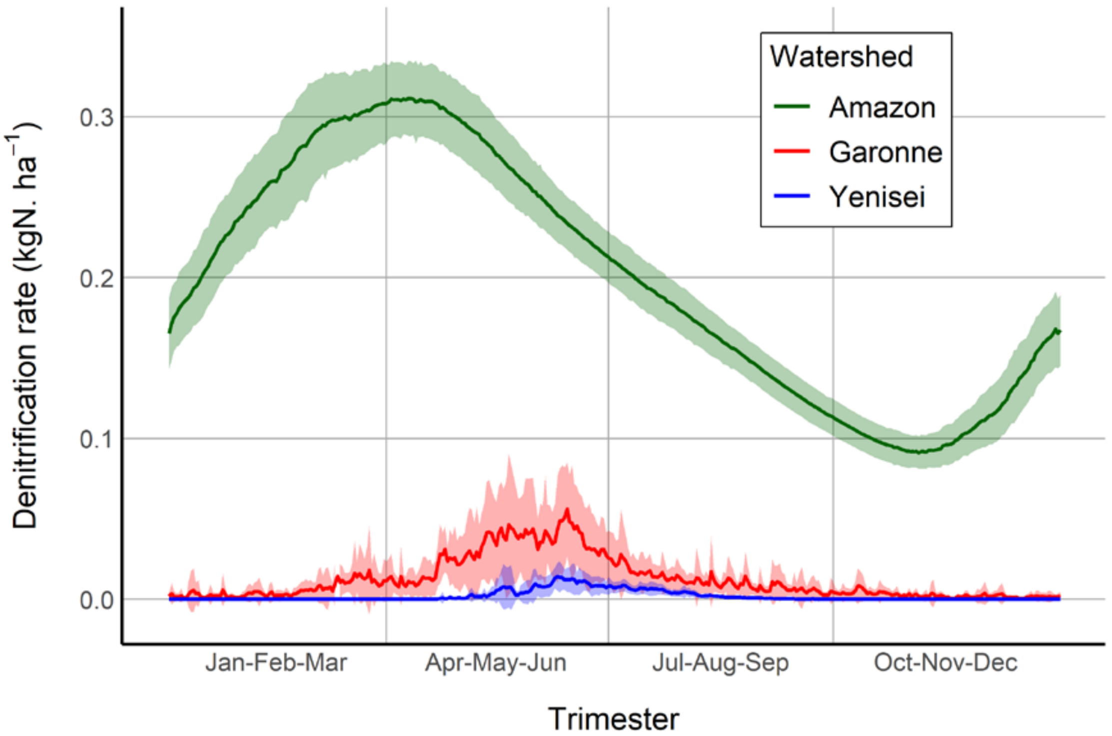

Figure 7: Average daily variations of the denitrification rates in the floodplains of the three selected watersheds on the period 2000-2010.

4 Discussion

4.1 Methodologies used

This paper exposed the capability of a simple model to describe daily denitrification rates in floodplains of contrasting watersheds. It is the first attempt to simulate, understand and compare daily denitrification rates in three different basins by applying a dynamic model. Previous large-scale denitrification models provided either estimation of interannual fluxes or assessed the denitrification contribution to the nitrogen budget (Birgand et al., 2007; Boyer et al., 2006; Groffman, 2012; Thouvenot-Korpoo et al., 2009). Others studies used models to estimate the denitrification at the global scale (Seitzinger et al., 2006). However, none have supplied daily denitrification rates yet. The need for a daily time step is important, particularly for basins subjected to sudden changes in the hydrological dynamic (as flash-flood in the Garonne River).

Compared to previous research, the model used in this paper was modified to integrate a new temperature dependence of R_{NO3} with an optimal set at 27°C. This term allowed the comparison of the denitrification rates between watersheds with different climates. This dependence is essential, especially for the Yenisei River, where the solutes are available, but the cold climate inhibits the microbial activity. Other studies mentioned an optimal temperature around 45°C for this process in soils (Benoit et al., 2015; Billen et al., 2018). More research is needed to better understand and consider this temperature effect in the proposed method.

The significant improvement of this model comes from the integration of the different carbon sources, together with nitrates as substrates, so that the stoichiometric ratio controls the denitrification rates. This operation was made possible with the help of C & N data sources with accurate temporal and spatial scales. The integration of the model of Fabre et al. (2019) to estimate the daily variations of DOC concentrations in the river as a source of C data to use for control of stoichiometric ratio the new model makes part of the new aspect. DOC plays a predominant role in the denitrification process. Therefore, the integration of the simulated DOC concentrations at a daily time step in the river is a notable improvement to refine denitrification estimates at the watershed scale.

The other part of the model concerned by the organic carbon integrates the role of the POC. POC was set up in the model depending on the average soils OC content of the three watersheds floodplains. A first improvement would be to spatialize more accurately the POC content at the subbasin scale. Therefore, more research should be conducted to validate global datasets of soil OC. Plus, the POC content used in this study does not consider the POC renewal by deposition during flooding events. The soil OC turnover may boost floodplain denitrification but was not studied yet.

Nonetheless, this model does not consider OC lability, which is essential in the estimation of denitrification rates (Zarnetske et al., 2011). Around 20% of the DOC is labile in freshwater ecosystems (Søndergaard and Middelboe, 1995; Guillemette and del Giorgio, 2011; McLaughlin and Kaplan, 2013). Integrating the lability in the denitrification model may improve

C and N dynamics in floodplains. Moreover, DOC is the most consumed form in denitrification (Peyrard et al., 2011; Zarnetske et al., 2011). Yet, the model does not integrate the dominant use of the DOC compared to the POC.

The delineation system from Rathjens et al. (2015) showed its capability to visualise the floodplains as a functional and active area. This tool could be further compared to remote sensing data from SWAF on the Amazon and other systems to see if easy-to-obtain data such as the DEM are sufficient to estimate floodplains coverage at the watershed scale.

Concerning the ratio between daily discharge and discharge at bank full depth, correction parameters were applied on the discharges at bank full depth based on known parts of the three watersheds. Uncertainties could remain in some other parts of the catchments, which would have a significant impact on the denitrification variations in surrounding areas. A better definition of discharge at bank full depth in the different parts of the basins may improve floodplains denitrification estimates at the watershed scale.

Moreover, we defined the mineralization rate constants for DOC and POC based on scarce in-situ measurements (Sun et al., 2018) which are non-representative of the entire watershed. Indeed, k_{POC} and k_{DOC} vary under the influence of multiple drivers such as soils characteristics, temperature and microorganism's activity (geophysical and biological characteristics). An improvement in the calculations of denitrification rates could be to measure these coefficients in different areas and determine their temporal and spatial variability in the floodplains. Concerning the half-saturation constant for nitrate limitation, this variable was based on in-situ observations in the Garonne hyporheic zone (Peyrard et al., 2011). Again, other measurements are needed to refine the value of K_{NO_3} in floodplains of various watersheds.

Lastly, this study outlines some weaknesses in the estimation of denitrification rates. Alluvial wetlands show higher denitrification than other areas in floodplains (McClain et al., 2003; Harrison et al., 2011). However, the model proposed here does not distinguish alluvial wetlands from the rest of the floodplains. Accurate mapping of alluvial wetlands at the watershed scale would help the scientific community to better estimate the specific denitrification rates in these highly reactive areas and consequently would improve the estimates in other areas of the floodplains.

4.2 Calibration of the inputs for denitrification

The concentrations of nutrients in floodplains were extracted from the SWAT model. This model, as shown in Table 1, already integrates denitrification processes. However, the denitrification represents the one occurring in uplands soils and stream but does not integrate the predominant role of floodplains aquifers (McClain et al., 2003). Therefore, our model proposed in this study could fill the gap and help to approach the floodplains denitrification contribution to N and C dynamics at the watershed scale.

This paper shows that the N and C inputs were calibrated successfully in different areas of the three watersheds. Nevertheless, these calibrations may be improved by better representing in-stream and uplands processes to improve the calibration of nitrate and organic carbon concentrations in floodplains aquifers. In the same way, nitrate concentrations in the Garonne River are underestimated and could induce lower denitrification.

Concerning OC, uncertainties remain in the simulation of DOC concentrations in the three watersheds on the one hand (Figure 5). Different processes and conditions are not considered in the model of Fabre et al. (2019) yet. Anthropogenic pressures in the Garonne River, as well as consumption, deposition, or floodplain deliveries for the Amazon River, are conditions that could explain the observed DOC variations. Process-based models could help to improve the DOC simulations by considering various in-stream processes such as in-stream assimilation or production (Du et al., 2020). However, DOC and nitrate concentrations are in the range of observations. Thus, the other components of the model regulate the denitrification rates on the Amazon River and the Garonne River.

On the other hand, the variations of observed DOC concentrations are so intense that the data quality could be discussed. Sampling nitrate and DOC in streams is difficult in large watersheds due to in-situ conditions. Thus, an improvement in the quality of data could be required to refine the parameters of the DOC model and to improve the modelling efforts for the nitrate concentrations or to confirm that the DOC model of Fabre et al. (2019) is adapted to various climatic and soils conditions.

4.3 Temporal and spatial validity of the resulting floodplains denitrification rates

We showed that even if the dynamics of nitrate and DOC concentrations in rivers are hard to obtain, these concentrations are in the range of observed data. Nevertheless, the concentrations at the outlet already integrate the complex processes occurring in the watershed. Consequently, we were able to extract from the SWAT model the average nitrate concentrations in the floodplains aquifers and compared it with the literature. In the Amazon watershed, the simulated nitrate concentrations in aquifers are around 0.9 ± 0.6 mgN-NO_3.L^{-1}. These values are in the range of the observations made in previous works (0.04-2.8 mgN-NO_3.L^{-1}; McClain et al., 1994; Leite et al., 2011). Concerning the Garonne basin, the SWAT model simulated average nitrate concentrations of 8.6 ± 5.8 mgN-NO_3.L^{-1} in aquifers while past research measured concentrations between 3.86 and 17.95 mgN-NO_3.L^{-1} (Jégo et al., 2012; Sun et al., 2018). The average nitrate concentrations in the Yenisei aquifers were far lower than the other basins with values around 0.01 ± 0.14 mgN-NO_3.L^{-1}. As no literature is available to validate these values in the Yenisei, we assumed that they are representative and could be used to estimate denitrification rates.

To validate our simulated denitrification rates, we compared our outputs with results from other studies in the same watersheds. Sánchez-Pérez et al. (2003) and Sun et al. (2018), based on in-situ observations, found that a highly reactive ecological corridor including efficient alluvial wetlands in the floodplains of the Garonne watershed provides a denitrification rate of 21-25 kgN-NO_3.ha^{-1}.yr^{-1}. On the same part of the watershed, our study gives a nitrate removal of 19.9 kgN-NO_3.ha^{-1}.yr^{-1}. Our rates are in the same order of magnitude, which could allow validating the method used in this paper.

We compared our results from the Amazon watershed with the estimation of Guilhen et al. (2020). This work focused on the three main floodplains of the Amazon: one alongside the mainstream near Obidos (station A1), one alongside the Branco and Negro rivers and one in the upstream Bolivian parts of the Madeira Basin. They found denitrification rates of 142.5 kgN.ha^{-1}.yr^{-1} on the mainstream floodplain, 38.8 kgN.ha^{-1}.yr^{-1} on the Branco floodplain and 60.4 kgN.ha^{-1}.yr^{-1} on the Madeira floodplain. In our study, we found denitrification rates of 165.7 kgN.ha^{-1}.yr^{-1} on the mainstream floodplain, 144.3 kgN.ha^{-1}.yr^{-1} on the Branco system and 67.6 kgN.ha^{-1}.yr^{-1} on the Madeira upstream part. Only the Branco floodplain shows different results. This offset could be due to different drivers influence. Guilhen et al. (2020) estimated the DOC concentrations at a monthly time step with high variations. In our study, the daily DOC concentrations are relatively constant but are still closer to the real concentrations. Their denitrification rates depend on the presence of water in the soil surface with a binary approach. In our study, the integration of the ratio between discharge and discharge at bank full depth improves the understanding of the denitrification dynamic. This improvement is not obvious in tropical systems such as the Amazon River because denitrification is occurring during the frequent and long-lasting flooding events. Therefore, our approach may be more relevant for basins where flooding events occur at a high temporal frequency, such as the Garonne River.

The temporal resolution of this study highlighted preferential periods of denitrification. For the three watersheds, the periods of high-water flows show a higher denitrification rate as implied by the model.

4.4 Efficiency of the different floodplains

By including contrasting watersheds, this paper brings to light a comparison of the efficiency of different types of floodplains with various anthropogenic and climatic contexts. Denitrification dynamics follow the hydrological cycles. Denitrification rates peak when and where both nitrate and DOC are not limiting factors like in the Amazon basin. On the contrary, the Garonne River has high exports of nitrate due to the anthropogenic pressures within the watershed. The DOC concentrations are always low except for some upstream parts of the watershed, which lead to higher denitrification rates. The Yenisei River has high DOC concentrations during the unfreezing period, but the low nitrate concentrations and the cold temperatures limit the denitrification. The suggested conceptualization integrates all of these contrasts between watersheds for the denitrification (Figure 8).

By comparing the average exports of nitrate and OC at the outlets of the three watersheds with the denitrification rates, we were able to evaluate the floodplains contribution to the regulating services of surface waters. The denitrification occurring in uplands and streams is already integrated into the flux exported to the oceans and is negligible compared to the one in floodplains. The DOC used for denitrification accounts for 10.4% of the total DOC flux exiting the Amazon basin (exported to the ocean or consumed by denitrification). This ratio reaches 3.0% in the Garonne and amounts to 0.9% for the Yenisei basin. Concerning nitrates, those processed in the denitrification represents 85% of the total nitrate flux exiting the Amazon basin and 34% in the Garonne watershed. For the Yenisei watershed, only 13% of the total nitrate flux exiting the basin is used for denitrification.

Concerning the Amazon and the Yenisei River, as the DOC concentrations are generally higher than nitrate, only a few of the total DOC yield is needed for the denitrification. The Garonne River, which is under high anthropogenic pressures, is characterized by soils with low organic matter contents and high exports of nitrates. The resulting concentrations in the river are quite in the same range, and a large part of the DOC export is needed to consume a small amount of the aquifers nitrate content.

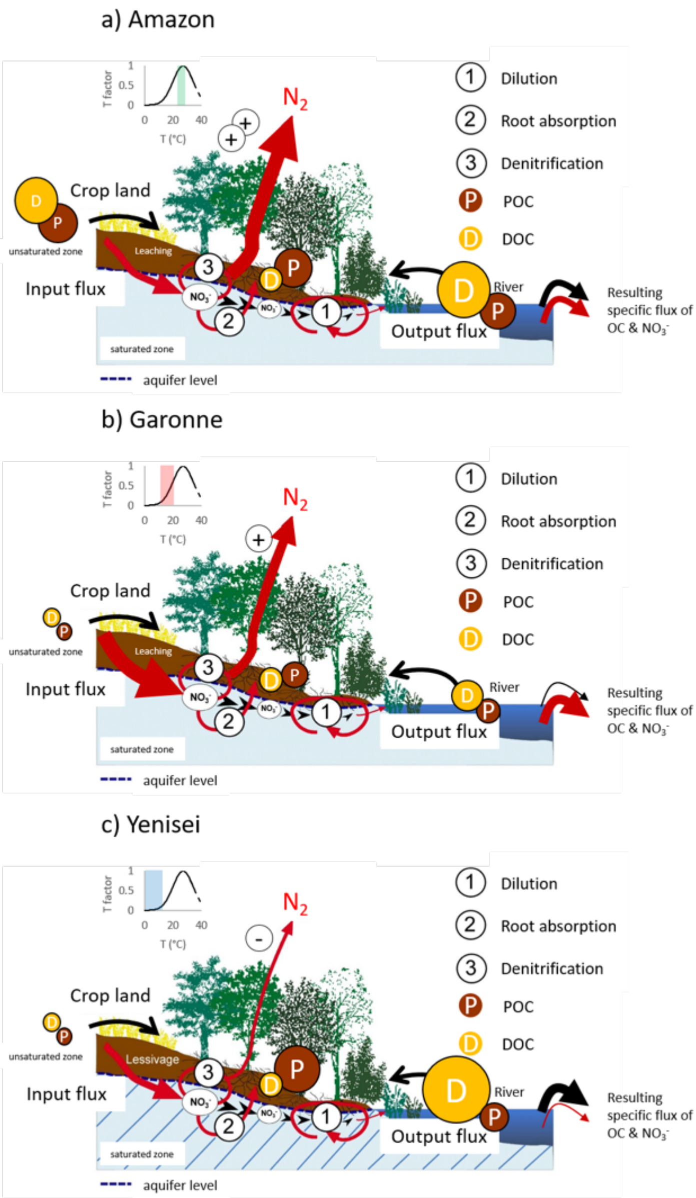

Figure 8: Conceptualization of the denitrification model for the selected watersheds. In each case of study, the different variables favouring the process shows various intensities. Adapted from Sánchez-Pérez and Trémolières (2003) and Bernard-Jannin et al. (2017). The red arrows represent nitrogen dynamics, and black arrows represent organic carbon pathways. The top-left graph shows the variation of the temperature index in the denitrification model. The coloured zones are the temperature intervals for each watershed.

5 Conclusion

This paper demonstrated the possibility of a simple model to simulate the floodplains denitrification rates in contrasting watersheds. We showed that tropical catchments that combine an average temperature around the optimal temperature for denitrification and large C availability show the highest amounts for the process. On the other hand, we confirmed that

C and N availability, as well as average temperature, could be limiting factors for floodplains denitrification on both cold and temperate watersheds. This study also highlighted the role of floodplains on water quality and their contribution to the stability and the resilience of the basins subjected to future climate and land use changes.

6 Acknowledgements

We do acknowledge the Observation Service SO HYBAM, the French Water Agency, Electricité De France (project REGARD-RTRA/STAE), Compagnie d'Aménagement des Coteaux de Gascogne, Banque Hydro, the Arctic Great Rivers Observatory and the TOMCAR-Permafrost Project for the sharing of their data on DOC, nitrate and daily discharge in the studied watersheds. This work is part of the governmental PhD program of Clément Fabre.

7 Authors contributions

C.F., J.G., S.S. and J.M.S.P. designed and developed the model with the help of R.C. C.F. performed and analyzed the modelling. C.F. wrote the paper with considerable contributions from J.M.S.P., S.S.; J.G., M.G. and R.C.

8 Additional information

This research did not receive any specific grant from funding agencies in the public, commercial, or not-for-profit sectors.

9 References

Arnold, J.G., Srinivasan, R., Muttiah, R.S., Williams, J.R., 1998. Large area hydrologic modelling and assessment part 1: model development. Journal of the American Water Resources Association 34, 73–89. https://doi.org/10.1111/j.1752-1688.1998.tb05961.x

Abril, G., Frankignoulle, M., 2001. Nitrogen–alkalinity interactions in the highly polluted Scheldt basin (Belgium). Water Research 35, 844–850. https://doi.org/10.1016/S0043-1354(00)00310-9

Baillieux, A., Campisi, D., Jammet, N., Bucher, S., Hunkeler, D., 2014. Regional water quality patterns in an alluvial aquifer: Direct and indirect influences of rivers. Journal of Contaminant Hydrology 169, 123–131. https://doi.org/10.1016/j.jconhyd.2014.09.002

Batjes, N.H., 2009. Harmonized soil profile data for applications at global and continental scales: updates to the WISE database. Soil Use and Management 25, 124–127. https://doi.org/10.1111/j.1475-2743.2009.00202.x

Benoit, M., Garnier, J., Billen, G., 2015. Temperature dependence of nitrous oxide production of a luvisolic soil in batch experiments. Process Biochemistry 50, 79–85. https://doi.org/10.1016/j.procbio.2014.10.013

Bernard-Jannin, L., Sun, X., Teissier, S., Sauvage, S., Sánchez-Pérez, J.-M., 2017. Spatio-temporal analysis of factors controlling nitrate dynamics and potential denitrification hot spots and hot moments in groundwater of an alluvial floodplain. Ecological Engineering 103, 372–384. https://doi.org/10.1016/j.ecoleng.2015.12.031

Billen, G., Garnier, J., Lassaletta, L., 2013. The nitrogen cascade from agricultural soils to the sea: modelling nitrogen transfers at regional watershed and global scales. Philosophical Transactions of the Royal Society B: Biological Sciences 368, 20130123–20130123. https://doi.org/10.1098/rstb.2013.0123

Billen, G., Ramarson, A., Thieu, V., Théry, S., Silvestre, M., Pasquier, C., Hénault, C., Garnier, J., 2018. Nitrate retention at the river–watershed interface: a new conceptual modelling approach. Biogeochemistry 139, 31–51. https://doi.org/10.1007/s10533-018-0455-9

Birgand, F., Skaggs, R.W., Chescheir, G.M., Gilliam, J.W., 2007. Nitrogen Removal in Streams of Agricultural Catchments—A Literature Review. Critical Reviews in Environmental Science and Technology 37, 381–487. https://doi.org/10.1080/10643380600966426

Boano, F., Demaria, A., Revelli, R., Ridolfi, L., 2010. Biogeochemical zonation due to intrameander hyporheic flow: Intrameander biogeochemical zonation. Water Resources Research 46. https://doi.org/10.1029/2008WR007583

Boyer, E.W., Alexander, R.B., Parton, W.J., Li, C., Butterbach-Bahl, K., Donner, S.D., Skaggs, R.W., Grosso, S.J.D., 2006. Modelling denitrification in terrestrial and aquatic ecosystems at regional scales. Ecological Applications 16, 2123–2142. https://doi.org/10.1890/1051-0761(2006)016[2123:MDITAA]2.0.CO;2

Brin, L.D., Giblin, A.E., Rich, J.J., 2017. Similar temperature responses suggest future climate warming will not alter partitioning between denitrification and anammox in temperate marine sediments. Global Change Biology 23, 331–340. https://doi.org/10.1111/gcb.13370

Cakir, R., Sauvage, S., Gerino, M., Volk, M., Sánchez-Pérez, J.M., 2020. Assessment of ecological function indicators related to nitrate under multiple human stressors in a large watershed. Ecological Indicators 111, 106016. https://doi.org/10.1016/j.ecolind.2019.106016

Canion, A., Overholt, W.A., Kostka, J.E., Huettel, M., Lavik, G., Kuypers, M.M.M., 2014. Temperature response of denitrification and anaerobic ammonium oxidation rates and microbial community structure in Arctic fjord sediments: Temperature and N cycling in Arctic sediments. Environmental Microbiology 16, 3331–3344. https://doi.org/10.1111/1462-2920.12593

Craig, L., Bahr, J.M., Roden, E.E., 2010. Localized zones of denitrification in a floodplain aquifer in southern Wisconsin, USA. Hydrogeology Journal 18, 1867–1879. https://doi.org/10.1007/s10040-010-0665-2

de Ferranti, J., Hormann, C., 2012. Digital Elevation Model.

Du, X., Loiselle, D., Alessi, D.S., Faramarzi, M., 2020. Hydro-climate and biogeochemical processes control watershed organic carbon inflows: Development of an in-stream organic carbon module coupled with a process-based hydrologic model. Science of The Total Environment 718, 137281. https://doi.org/10.1016/j.scitotenv.2020.137281

EEA Report, 2013. UWWTD data sources [WWW Document]. European Environment Agency. URL: https://www.eea.europa.eu/themes/water/european-waters/water-use-and-environmental-pressures/uwwtd/uwwtd-data-sources (accessed 11.27.18).

Elmi, A.A., Madramootoo, C., Hamel, C., Liu, A., 2003. Denitrification and nitrous oxide to nitrous oxide plus dinitrogen ratios in the soil profile under three tillage systems. Biology and Fertility of Soils 38, 340–348. https://doi.org/10.1007/s00374-003-0663-9

European Commission, 2003. Global Land Cover 2000 database.

Fabre, C., Sauvage, S., Tananaev, N., Srinivasan, R., Teisserenc, R., Sánchez Pérez, J., 2017. Using Modeling Tools to Better Understand Permafrost Hydrology. Water 9, 418. https://doi.org/10.3390/w9060418

Fabre, C., Sauvage, S., Tananaev, N., Noël, G.E., Teisserenc, R., Probst, J.L., Sánchez-Pérez, J.M., 2019. Assessment of sediment and organic carbon exports into the Arctic ocean: The case of the Yenisei River basin. Water Research 158, 118–135. https://doi.org/10.1016/j.watres.2019.04.018

Ferrant, S., Oehler, F., Durand, P., Ruiz, L., Salmon-Monviola, J., Justes, E., Dugast, P., Probst, A., Probst, J.-L., Sanchez-Perez, J.-M., 2011. Understanding nitrogen transfer dynamics in a small agricultural catchment: Comparison of a distributed (TNT2) and a semi-distributed (SWAT) modelling approaches. Journal of Hydrology 406, 1–15. https://doi.org/10.1016/j.jhydrol.2011.05.026

Friedl, J., Scheer, C., Rowlings, D.W., McIntosh, H.V., Strazzabosco, A., Warner, D.I., Grace, P.R., 2016. Denitrification losses from an intensively managed sub-tropical pasture – Impact of soil moisture on the partitioning of N 2 and N 2 O emissions. Soil Biology and Biochemistry 92, 58–66. https://doi.org/10.1016/j.soilbio.2015.09.016

Fu, B., Merritt, W.S., Croke, B.F.W., Weber, T.R., Jakeman, A.J., 2019. A review of catchment-scale water quality and erosion models and a synthesis of future prospects. Environmental Modelling & Software 114, 75–97. https://doi.org/10.1016/j.envsoft.2018.12.008

Gift, D.M., Groffman, P.M., Kaushal, S.S., Mayer, P.M., 2010. Denitrification Potential, Root Biomass, and Organic Matter in Degraded and Restored Urban Riparian Zones. Restoration Ecology 18, 113–120. https://doi.org/10.1111/j.1526-100X.2008.00438.x

Groffman, P.M., 2012. Terrestrial denitrification: challenges and opportunities. Ecological Processes 1. https://doi.org/10.1186/2192-1709-1-11

Groffman, P.M., Altabet, M.A., Böhlke, J.K., Butterbach-Bahl, K., David, M.B., Firestone, M.K., Giblin, A.E., Kana, T.M., Nielsen, L.P., Voytek, M.A., 2006. Methods for measuring denitrification: diverse approaches to a difficult problem. Ecological Applications 16, 2091–2122. https://doi.org/10.1890/1051-0761(2006)016[2091:MFMDDA]2.0.CO;2

Groffman, P.M., Butterbach-Bahl, K., Fulweiler, R.W., Gold, A.J., Morse, J.L., Stander, E.K., Tague, C., Tonitto, C., Vidon, P., 2009. Challenges to incorporating spatially and temporally explicit phenomena (hotspots and hot moments) in denitrification models. Biogeochemistry 93, 49–77. https://doi.org/10.1007/s10533-008-9277-5

Guilhen, J., Al Bitar, A., Sauvage, S., Parrens, M., Martinez, J.-M., Abril, G., Moreira-Turcq, P., Sanchez-Pérez, J.-M., 2020. Denitrification, carbon and nitrogen emissions over the

Amazonianwetlands (preprint). Biogeochemistry: Wetlands. https://doi.org/10.5194/bg-2020-3

Guillemette, F., del Giorgio, P.A., 2011. Reconstructing the various facets of dissolved organic carbon bioavailability in freshwater ecosystems. Limnology and Oceanography 56, 734–748. https://doi.org/10.4319/lo.2011.56.2.0734

Harrison, M.D., Groffman, P.M., Mayer, P.M., Kaushal, S.S., Newcomer, T.A., 2011. Denitrification in Alluvial Wetlands in an Urban Landscape. Journal of Environmental Quality 40, 634–646. https://doi.org/10.2134/jeq2010.0335

Hattermann, F.F., Krysanova, V., Habeck, A., Bronstert, A., 2006. Integrating wetlands and riparian zones in river basin modelling. Ecological Modelling 199, 379–392. https://doi.org/10.1016/j.ecolmodel.2005.06.012

Helton, A.M., Poole, G.C., Payn, R.A., Izurieta, C., Stanford, J.A., 2014. Relative influences of the river channel, floodplain surface, and alluvial aquifer on simulated hydrologic residence time in a montane river floodplain. Geomorphology 205, 17–26. https://doi.org/10.1016/j.geomorph.2012.01.004

Holmes, R.M., McClelland, J.W., Tank, S.E., Spencer, R.G.M., Shiklomanov, A.I. 2018. Arctic Great Rivers Observatory. Water Quality Dataset. https://www.arcticgreatrivers.org/data

Hope, D., Billett, M.F., Cresser, M.S., 1994. A review of the export of carbon in river water: Fluxes and processes. Environmental Pollution 84, 301–324. https://doi.org/10.1016/0269-7491(94)90142-2

Jégo, G., Sánchez-Pérez, J.M., Justes, E., 2012. Predicting soil water and mineral nitrogen contents with the STICS model for estimating nitrate leaching under agricultural fields. Agricultural Water Management 107, 54–65. https://doi.org/10.1016/j.agwat.2012.01.007

Jung, G., Wagner, S., Kunstmann, H., 2012. Joint climate–hydrology modelling: an impact study for the data-sparse environment of the Volta Basin in West Africa. Hydrology Research 43, 231–248. https://doi.org/10.2166/nh.2012.044

Leite, N.K., Krusche, A.V., Cabianchi, G.M., Ballester, M.V.R., Victoria, R.L., Marchetto, M., Santos, J.G. dos, 2011. Groundwater quality comparison between rural farms and riparian wells in the western Amazon, Brazil. Química Nova 34, 11–15. https://doi.org/10.1590/S0100-40422011000100003

Lu, J.Z., Zhang, L., Cui, X.L., Zhang, P., Chen, X.L., Sauvage, S., Sanchez-Perez, J.M., 2019. Assessing the climate forecast system reanalysis weather data-driven hydrological model for the Yangtze river basin in China. Applied Ecology and Environmental Research 17, 3615–3632. https://doi.org/10.15666/aeer/1702_36153632

Mayorga, E., Seitzinger, S.P., Harrison, J.A., Dumont, E., Beusen, A.H.W., Bouwman, A.F., Fekete, B.M., Kroeze, C., Van Drecht, G., 2010. Global Nutrient Export from WaterSheds 2 (NEWS 2): Model development and implementation. Environmental Modelling & Software 25, 837–853. https://doi.org/10.1016/j.envsoft.2010.01.007

McClain, M., Richey, J., Pimentel, T., 1994. Groundwater nitrogen dynamics at the terrestrial-lotic interface of a small catchment in the Central Amazon basin. Biogeochemistry 27. https://doi.org/10.1007/BF00002814

McClain, M.E., Boyer, E.W., Dent, C.L., Gergel, S.E., Grimm, N.B., Groffman, P.M., Hart, S.C., Harvey, J.W., Johnston, C.A., Mayorga, E., McDowell, W.H., Pinay, G., 2003. Biogeochemical Hot Spots and Hot Moments at the Interface of Terrestrial and Aquatic Ecosystems. Ecosystems 6, 301–312. https://doi.org/10.1007/s10021-003-0161-9

McLaughlin, C., Kaplan, L.A., 2013. Biological lability of dissolved organic carbon in stream water and contributing terrestrial sources. Freshwater Science 32, 1219–1230. https://doi.org/10.1899/12-202.1

Meybeck, M., 1993. C, N, P and S in Rivers: From Sources to Global Inputs, in: Wollast, R., Mackenzie, F.T., Chou, L. (Eds.), Interactions of C, N, P and S Biogeochemical Cycles and Global Change. Springer Berlin Heidelberg, Berlin, Heidelberg, pp. 163–193.

Moriasi, D.N., Arnold, J.G., Liew, M.W.V., Bingner, R.L., Harmel, R.D., Veith, T.L., 2007. Model Evaluation Guidelines for Systematic Quantification of Accuracy in Watershed Simulations. Transactions of the ASABE 50, 885–900. https://doi.org/10.13031/2013.23153

Moriasi, D.N., Gitau, M.W., Pai, N., Daggupati, P., 2015. Hydrologic and Water Quality Models: Performance Measures and Evaluation Criteria. Transactions of the ASABE 58, 1763–1785. https://doi.org/10.13031/trans.58.10715

Observation Service SO HYBAM, n.d. Observation Service for the geodynamical, hydrological and biogeochemical control of erosion/alteration and material transport in the Amazon, Orinoco and Congo basins.

Oeurng, C., Sauvage, S., Sánchez-Pérez, J.-M., 2011. Assessment of hydrology, sediment and particulate organic carbon yield in a large agricultural catchment using the SWAT model. Journal of Hydrology 401, 145–153. https://doi.org/10.1016/j.jhydrol.2011.02.017

Parrens, M., Al Bitar, A., Frappart, F., Papa, F., Calmant, S., Crétaux, J.-F., Wigneron, J.-P., Kerr, Y., 2017. Mapping Dynamic Water Fraction under the Tropical Rain Forests of the Amazonian Basin from SMOS Brightness Temperatures. Water 9, 350. https://doi.org/10.3390/w9050350

Parrens, M., Kerr, Y., Al Bitar, A., 2018. SWAF-HR: A High Spatial and Temporal Resolution Water Surface Extent Product Over the Amazon Basin, in: IGARSS 2018 - 2018 IEEE International Geoscience and Remote Sensing Symposium. Presented at the IGARSS 2018 - 2018 IEEE International Geoscience and Remote Sensing Symposium, IEEE, Valencia, pp. 8389–8392. https://doi.org/10.1109/IGARSS.2018.8519079

Parrens, M., Al Bitar, A.A., Frappart, F., Paiva, R., Wongchuig, S., Papa, F., Yamasaki, D., Kerr, Y., 2019. High-resolution mapping of inundation area in the Amazon basin from a combination of L-band passive microwave, optical and radar datasets. International Journal of Applied Earth Observation and Geoinformation 81, 58–71. https://doi.org/10.1016/j.jag.2019.04.011

Peter, S., Koetzsch, S., Traber, J., Bernasconi, S.M., Wehrli, B., Durisch-Kaiser, E., 2012. Intensified organic carbon dynamics in the groundwater of a restored riparian zone: Organic carbon in riparian aquifers. Freshwater Biology 57, 1603–1616. https://doi.org/10.1111/j.1365-2427.2012.02821.x

Peyrard, D., Delmotte, S., Sauvage, S., Namour, P., Gerino, M., Vervier, P., Sanchez-Perez, J.M., 2011. Longitudinal transformation of nitrogen and carbon in the hyporheic zone of an N-rich stream: A combined modelling and field study. Physics and Chemistry of the Earth, Parts A/B/C 36, 599–611. https://doi.org/10.1016/j.pce.2011.05.003

Pfeiffer, S.M., Bahr, J.M., Beilfuss, R.D., 2006. Identification of groundwater flow paths and denitrification zones in a dynamic floodplain aquifer. Journal of Hydrology 325, 262–272. https://doi.org/10.1016/j.jhydrol.2005.10.019

Pinay, G., Ruffinoni, C., Wondzell, S., Gazelle, F., 1998. Change in Groundwater Nitrate Concentration in a Large River Floodplain: Denitrification, Uptake, or Mixing? Journal of the North American Benthological Society 17, 179–189. https://doi.org/10.2307/1467961

Ranalli, A.J., Macalady, D.L., 2010. The importance of the riparian zone and in-stream processes in nitrate attenuation in undisturbed and agricultural watersheds – A review of the scientific literature. Journal of Hydrology 389, 406–415. https://doi.org/10.1016/j.jhydrol.2010.05.045

Rathjens, H., Oppelt, N., Bosch, D.D., Arnold, J.G., Volk, M., 2015. Development of a grid-based version of the SWAT landscape model: Development of a grid-based version of the

SWAT landscape model. Hydrological Processes 29, 900–914. https://doi.org/10.1002/hyp.10197

Raymond, P.A., Bauer, J.E., 2001. Use of 14 C and 13 C natural abundances for evaluating riverine, estuarine, and coastal DOC and POC sources and cycling: a review and synthesis. Organic Geochemistry 32, 469–485. https://doi.org/10.1016/S0146-6380(00)00190-X

Rivett, M.O., Buss, S.R., Morgan, P., Smith, J.W.N., Bemment, C.D., 2008. Nitrate attenuation in groundwater: A review of biogeochemical controlling processes. Water Research 42, 4215–4232. https://doi.org/10.1016/j.watres.2008.07.020

Ruelland, D., Billen, G., Brunstein, D., Garnier, J., 2007. SENEQUE: A multi-scaling GIS interface to the Riverstrahler model of the biogeochemical functioning of river systems. Science of The Total Environment 375, 257–273. https://doi.org/10.1016/j.scitotenv.2006.12.014

Saad, O.A.L.O., Conrad, R., 1993. Temperature dependence of nitrification, denitrification, and turnover of nitric oxide in different soils. Biology and Fertility of Soils 15, 21–27. https://doi.org/10.1007/BF00336283

Sánchez-Pérez, J.M., Trémolières, M., 2003. Change in groundwater chemistry as a consequence of suppression of floods: the case of the Rhine floodplain. Journal of Hydrology 270, 89–104. https://doi.org/10.1016/S0022-1694(02)00293-7

Sánchez-Pérez, J.M., Vervier, P., Garabétian, F., Sauvage, S., Loubet, M., Rols, J.L., Bariac, T., Weng, P., 2003. Nitrogen dynamics in the shallow groundwater of a riparian wetland zone of the Garonne, SW France: nitrate inputs, bacterial densities, organic matter supply and denitrification measurements. Hydrology and Earth System Sciences Discussions 7, 97–107.

Sauvage, S., Sánchez-Pérez, J.-M., Vervier, P., Naiman, R.-J., Alexandre, H., Bernard-Jannin, L., Boulêtreau, S., Delmotte, S., Julien, F., Peyrard, D., Sun, X., Gerino, M., 2018. Modelling the role of riverbed compartments in the regulation of water quality as an ecological service. Ecological Engineering 118, 19–30. https://doi.org/10.1016/j.ecoleng.2018.02.018

Seitzinger, S., Harrison, J.A., Böhlke, J.K., Bouwman, A.F., Lowrance, R., Peterson, B., Tobias, C., Drecht, G.V., 2006. Denitrification across landscapes and waterscapes: a synthesis. Ecological Applications 16, 2064–2090. https://doi.org/10.1890/1051-0761(2006)016[2064:DALAWA]2.0.CO;2

Smith, K., 1997. The potential for feedback effects induced by global warming on emissions of nitrous oxide by soils. Global Change Biology 3, 327–338. https://doi.org/10.1046/j.1365-2486.1997.00100.x

Søndergaard, M., Middelboe, M., 1995. A cross-system analysis of labile dissolved organic carbon. Marine Ecology Progress Series 118, 283–294. https://doi.org/10.3354/meps118283

Sun, X., 2015. Modélisation des échanges nappe-rivière et du processus de dénitrification dans les plaines alluviales à l'échelle du bassin versant (PhD Thesis).

Sun, X., Bernard-Jannin, L., Grusson, Y., Sauvage, S., Arnold, J., Srinivasan, R., Sánchez-Pérez, J., 2018. Using SWAT-LUD Model to Estimate the Influence of Water Exchange and Shallow Aquifer Denitrification on Water and Nitrate Flux. Water 10, 528. https://doi.org/10.3390/w10040528

Tenuta, M., Sparling, B., 2011. A laboratory study of soil conditions affecting emissions of nitrous oxide from packed cores subjected to freezing and thawing. Canadian Journal of Soil Science 91, 223–233. https://doi.org/10.4141/cjss09051

Thouvenot-Korppoo, M., Billen, G., Garnier, J., 2009. Modelling benthic denitrification processes over a whole drainage network. Journal of Hydrology 379, 239–250. https://doi.org/10.1016/j.jhydrol.2009.10.005

Yamazaki, D., Kanae, S., Kim, H., Oki, T., 2011. A physically-based description of floodplain inundation dynamics in a global river routing model: Floodplain inundation dynamics. Water Resources Research 47. https://doi.org/10.1029/2010WR009726

Zaman, M., Nguyen, M.L., Simek, M., Nawaz, S., Khan, M.J., Babar, M.N., Zaman, S., 2012. Emissions of nitrous oxide (N_2O) and dinitrogen (N_2) from the agricultural landscapes, sources, sinks, and factors affecting N_2O and N_2 ratios, in: Greenhouse Gases-Emission, Measurement and Management. IntechOpen.

Zarnetske, J.P., Haggerty, R., Wondzell, S.M., Baker, M.A., 2011. Labile dissolved organic carbon supply limits hyporheic denitrification. Journal of Geophysical Research 116. https://doi.org/10.1029/2011JG001730

Zarnetske, J.P., Haggerty, R., Wondzell, S.M., Bokil, V.A., González-Pinzón, R., 2012. Coupled transport and reaction kinetics control the nitrate source-sink function of hyporheic zones: Hyporheic N source-sink controls. Water Resources Research 48. https://doi.org/10.1029/2012WR011894

10 Appendices

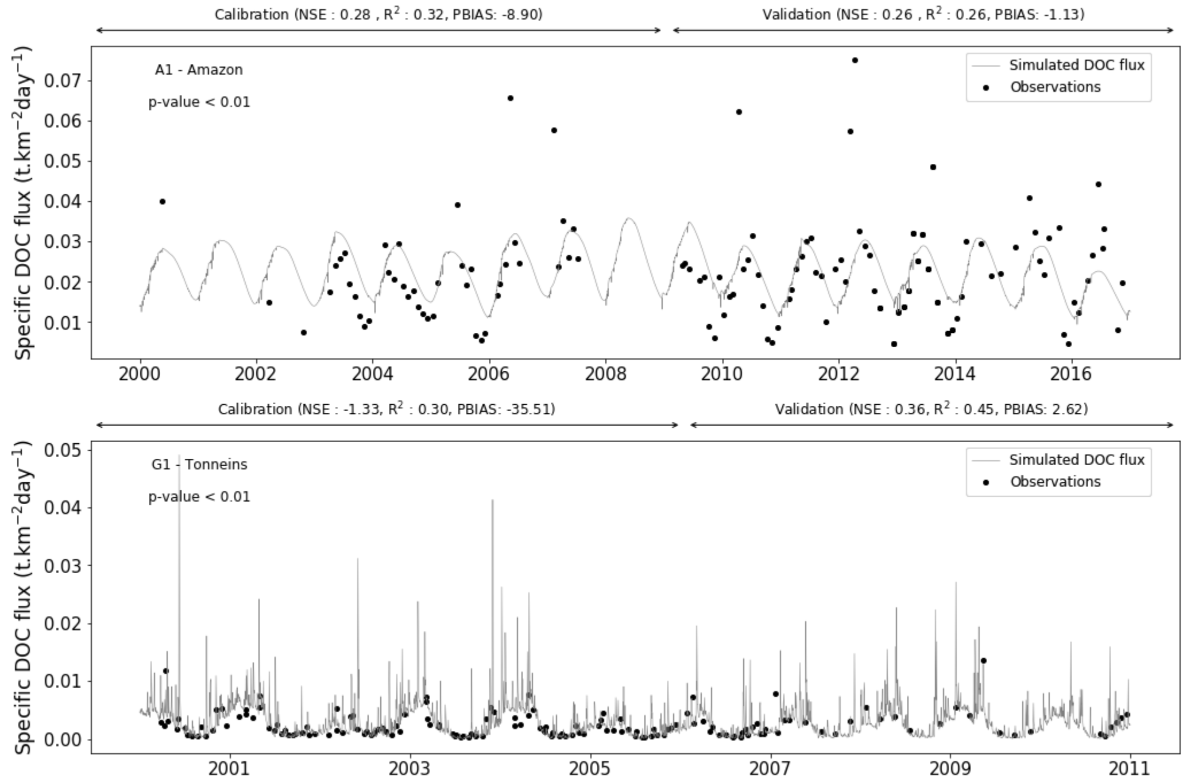

Appendix 1: Daily DOC fluxes exported at the outlet of a) the Amazon River, b) the Garonne River and c) the Yenisei River. The Yenisei graph is adapted from Fabre et al. (2019). Locations of the sampling stations are found in Figure 1.